Research Article

Synthesis of TiO_2 nanoparticles by chemical and green synthesis methods and their multifaceted properties

M. Aravind[1,3] · M. Amalanathan[1,3] · M. Sony Michael Mary[2,3]

Received: 18 September 2020 / Accepted: 27 January 2021 / Published online: 3 March 2021

Abstract
In this present work, Titanium dioxide nanoparticles (TiO_2 NPs) successfully synthesized using the chemical as well as the green synthesis routine. The ethanol provoked the chemical reduction of ions. In the green synthesis, jasmine flower extract was used as a reducing and stabilizing agent because it contains alkaloids, coumarins, flavonoids. The Rutile phase of TiO_2 NPs with an average crystalline size of 31–42 nm was revealed from the XRD pattern. From the UV–Visible spectroscopy, the optically active region of TiO_2 NPs at 385 nm represents the visible region spectrum. The Ti–O–Ti and Ti–O vibration bond formation confirms the formation of TiO_2 NPs. The SEM image of TiO_2 NPs reveals that the spherical shaped NPs with randomly arranged manner. The obtained results have revealed that the property of TiO_2 nanoparticles was similar in both processes. The Photodegradation of methylene blue dye was investigated and resulted in the maximum degradation efficiency of 92% is achieved at 120 min of irradiation. The Photodegradation study shows the biosynthesized TiO_2 NPs exhibits a higher degradation efficiency compared to chemically synthesized TiO_2 NPs. The antibacterial activity of prepared TiO_2 NP's was studied using grams-positive and gram-negative strains. The biological activities of green synthesized TiO_2 NPs are enhanced compared to the chemically synthesized TiO_2 NPs. Hence the degradation efficiency and zone inhibition layer indicate that the prepared TiO_2 NPs are the potential candidate for environmental and biomedical applications.

Graphic abstract

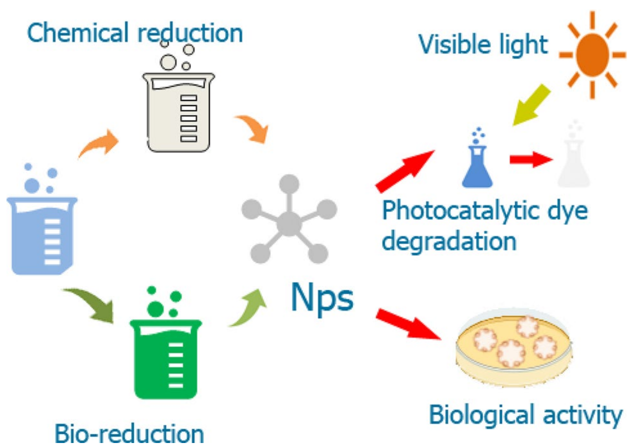

✉ M. Amalanathan, nathan.amalphysics@gmail.com | [1]Research Scholar, Department of Physics, Nanjil Catholic College of Arts and Science, Kaliyakkavilai, Kanyakumari, Tamil Nadu, India. [2]Research Scholar, Nesamony Memorial Christian College Marthandam, Kanyakumari, Tamil Nadu, India. [3]Affiliated to Manonmaniam Sundaranar University, Abishekapatti, Tirunelveli, Tamil Nadu 627012, India.

SN Applied Sciences (2021) 3:409 | https://doi.org/10.1007/s42452-021-04281-5

Keywords Titanium dioxide · Jasmine flower · Hydrothermal method · Methylene blue · Antibacterial activity

1 Introduction

Nanomaterials belongs to the range of below 100 nm has unique chemical, physical, electrical, and mechanical properties and also diversely utilized in the field of medical, biotechnology, microbiology, pharmaceutics and chemistry, engineering, inexpensive catalyst, cytotoxicity study, etc. [1–3]. Owing to its large surface area, nanomaterial synthesis methods are classified into the physical and chemical methods. However, these methods are not suitable for medicinal and biological applications because of its harmful nature to the environment. Therefore, researchers are going for a green synthesis route to prepare nanomaterials because the green synthesis approach is simple, eco-friendly, and cost-effective [4, 5]. Green synthesis is a fascinating method for material science [6–8].In the past few decades, metal oxide semiconductors such as ZnO, MgO, CuO, CdO, NiO, etc. were widely used, and it is prepared via physical, chemical, and biological methods. Among them, TiO_2 NPs are a well-known semiconductor with a wide bandgap of 3.2 eV for anatase and 3.0 eV for rutile phase [9], but the brookite phase is rare to obtain [10]. The Anatase and rutile phase of TiO_2 exhibits a tetragonal crystal structure, but the brookite phase is an orthorhombic structure [11]. The transition metal oxide, mainly TiO_2, is widely used in cosmetics, photocatalysts, medicines, sensors, and solar cell applications because of its peculiar properties like interconnected pores and large surface area [12].

Nowadays, the metal and metal oxide nanoparticles are synthesized by chemical as well as physical methods such as the microwave [13], hydrothermal [14], solid-state [15], solution route method [16], sol–gel [17] chemical phase decomposition vapour [18], solvothermal crystallization [19], ultrasonic irradiation and [20], and green synthesis method [21]. Nevertheless, these methods generate heterogeneous NPs with high energy consumption and also the chemicals process involves synthetic capping, reducing, and stabilizing agents which results in the creation of anti-environmentally safe by-products [22]. In recent years researchers are focussed on the green synthesis route to the synthesis of metal and metal oxide nanoparticles. The bio-mediated metal and metal oxide NP's shows potential application on drug delivery, nanocatalyst, nano-medicine, biosensor, biotechnology, and microbiology. The green synthesis method is similar to the chemical reduction process, where the costly chemical reagents are replaced by plant extracts and microorganisms and also reduces the toxicity, which enhances its biomedical applications.

The bio-mediated TiO_2 NPs exhibit excellent antibacterial, anti-inflammatory, anti-fungal, anti-microbial, and several biological activities. The decomposition of micro-organisms by its photo-semiconductor properties results in the enhancement of biological activities [23]. There are numerous reports on the preparation of TiO_2 NPs from *Cinnamon Powder* [9], *Mangifera indica* [24] *Citrus reticulate* [25] *Azadirachtaindica leaf* [26] *Murayakoenigii* [27] *Curcuma longa* [28], *Cynodondactylon* [1], *Annona squamosa* [29], *Morindacitrifolia* [30], *Psidium guajava* [31], *Jatropha curcas* [32], *Fungus-mediated* [33] towards the biological applications. Moreover, the morphology, size, shape, porosity, and crystallinity depend upon the concentration of precursor and temperature [34].

This present study is to investigate the chemical and bio-synthesis of the TiO_2 nanoparticles. The phytochemicals present in jasmine flower extracts are alkaloids, coumarins, flavonoids, tannins, terpenoids, glycosides, embodies, steroids, essential oil, and saponins [35]. These phytochemicals are responsible for the reduction of Titanium tetra Isopropoxide to titanium dioxide nanoparticles. The structural, morphological, vibrational, and optical properties of the TiO_2 NPs were analyzed. The photodegradation of methylene blue dye were visualized uisng UV-Visible irradiation technique. As well as the antibacterial activity were tested against both gram-positive and gram-negative strains . The different processes of TiO_2 nanoparticles synthesis were studied in detail.

2 Materials and methods

2.1 Materials

Titanium Tetra Isopropoxide (TTIP, $C_{12}H_{28}O_4Ti$, 97%), Ethanol (C_2H_5OH, 96%), Methylene blue ($C_{16}H_{18}ClN_3S$), and distilled water was purchased from Merck India. Jasmine flowers were collected from the local market. All chemicals and reagents are of analytic grade and used without further purification. Bacterial pathogens, such as Staphylococcus aureus (gram-positive bacteria), Klebsiella pneumonia and E-coli (gram-negative bacteria) were used to study biological activities.

2.2 Synthesis of TiO_2 by hydrothermal method

The slight modifications were made on the synthesis of TiO_2 NPs from the previously reported literature [36]. Initially, 0.1 N of titanium tetra isopropoxide is dissolved in 20 ml of ethanol solution under continuous stirring for

30 min. After that, add a few drops of distilled water to form the dispersion medium. The product was placed on the ultrasonic bath for 20 min. After sonication, the solution was transferred into an autoclave at 150 °C for 3 h. Then the solution was cool to room temperature, and it was washed and centrifuged with deionized water to remove the impurities. Then it is filtered with Whatman No. 1 Filter paper. The filtered sample was dried oven at 110 °C for 5 h, and it is further annealed at 500 °C for 2 h. The resultant TiO_2 NPs was collected and processed with further characterization.

2.3 Green synthesis of TiO_2 nanoparticles using jasmine flower extract

TiO_2 NPs were synthesized using the facile green synthesis route from Jasmine flower extract acts as a reducing/capping agent. The jasmine flowers were purchased from the local market of Nagercoil, Tamilnadu. The jasmine flower extract was prepared by adding 50 g of jasmine flower in 100 ml distilled water and boiled the mixture with a hotplate for 30 min. Then the aqueous solution has been filtered and stored for further tests. Take 50 ml of titanium tetra isopropoxide (TTIP) in a 100 ml beaker and add 20 ml of flower extract drop by drop to the above TTIP solution. The solution was stirred by 3 h at room temperature. The colour of the solution was changed from pure white to yellowish-grey. A change of colour confirms the formation of titanium dioxide nanoparticles. After that, the solution was Filter and dried at 110 °C for 5 h. Then the dried samples were calcined Muffle furnace at 500 °C for 2 h [37, 38].

2.4 Characterization of TiO_2 nanoparticles

X-Ray Diffraction pattern of investigated titanium dioxide nanoparticles was recorded by using PANanalytical XPERT PRO Diffractometer. FT-IR spectrum was recorded by using the Perkin Elmer spectrophotometer recorded from 400 to 4000 cm^{-1}. The Surface morphology of TiO_2 nanoparticles was visualized using SEM. EDS spectrum is used to determine its homogeneity and its elemental distribution of elements in the investigated compound. SEM with EDS spectrum was recorded with the help of Quanta FEG-250. UV–Visible Diffuse Reflectance Spectrophotometer (DRS) spectrum was recorded using a Shimadzu 2700 spectrophotometer. The reflectance spectrum was recorded in the range of 200–800 nm. The antibacterial activity of TiO_2 nanoparticles was studied for both gram-positive and gram-negative bacteria by the disk diffusion method.

2.5 Antibacterial activity

The antibacterial activity of titanium dioxide nanoparticles was tested by the agar diffusion method. First, the nutrient agar was uniformly spread in the Petri dish plate. Then fix the 6 mm diameter well, which is used to study the inhibition zone. Place 50 µl of TiO_2 NPs in 6 mm diameter well. The culture medium was incubated at 37 °C C for 24 h under aerobic conditions. The zone of inhibition layer was measured using the millimeter region. The Zone of inhibition results in the antibacterial activity of TiO_2 NPs.

2.6 Photodegradation of Methylene blue

Methylene blue dye is used as a model pollutant for photodegradation. Take 100 mg of TiO_2 NPs in 250 ml beaker with contains 100 ml methylene blue solution under ultrasonication for 20 min. Furthermore, the mixed solution was kept in a chamber at the dark condition to attain the absorption desorption equilibrium. The photodegradation of methylene blue dye was recorded with the help of UV–Visible irradiation at every 30 min regular interval from 0 to 120 min. The absorbance of methylene blue dye was recorded using 200 µl volume and 10 cm length quartz cuvette. Then the dye degradation efficiency was calculated.

3 Results and discussion

3.1 X-Ray Diffraction

The X-ray diffraction technique analyzed the crystalline phase, crystal structure, purity, and average crystalline size of the TiO_2 NPs. Figure 1 displays the XRD pattern

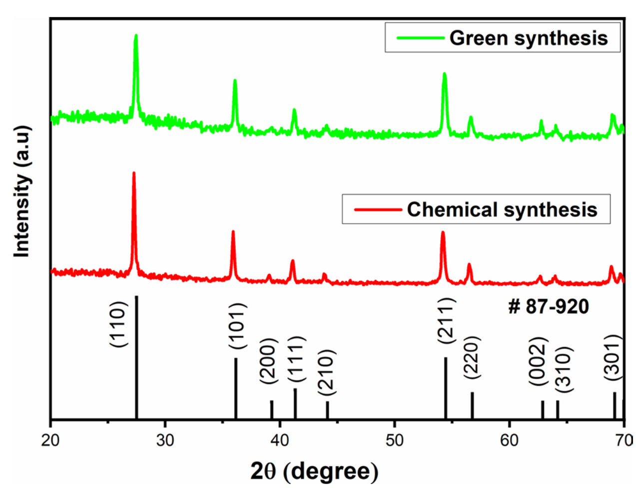

Fig. 1 Shows XRD pattern of TiO_2 nanoparticles

of bio mediated and chemically synthesized TiO_2 NPs. The diffraction angle (2Θ) at 27.45°,36.75°,41.27°, 44.07°, 54.27°, 56.54°, 62.78°, 64.05°, 69.01°, and 69.85° which corresponds to the Braggs reflection plane of (110), (101), (111), (210), (211), (220), (002), and (301) respectively. The observed angle at 27.45° (101) represents the high crystalline nature of TiO_2 NPs. The XRD pattern of TiO_2 NPs shows good agreement with the JCPDS card number: 89-4920, and it exhibits the tetragonal crystal structure [39]. The average crystalline size of TiO_2 NPs was calculated from the XRD pattern using the Debye Scherer formula

$$D = k\lambda/\beta \cos\theta,$$

where D is an average crystalline size, K is a dimensionless shape factor with a value close to unity, λ is the wavelength of the X-ray, β is the full width half the maximum intensity (FWHM) and θ is the Bragg angle [40, 41]. The average crystalline size of TiO_2 NPs was found in the range of 31–42 nm. Observed average crystalline size values well-matched with previous reports [42–44]. However, there is a small difference in peak strength, phase shift, and average crystalline size due to the synthesis process. The green TiO_2 nanoparticles were exhibited higher intensity TiO_2 peaks due to the presence of polyphenolic compounds in the plant extract. XRD data were tabulated in Table 1.

3.2 Fourier transform infrared spectroscopy

The functional group and chemical compound present in the prepared TiO_2 NPs were identified using the FT–IR spectrum. Figure 2 shows the FT–IR spectrum of TiO_2 NPs. The broadband at 3709–3712 cm^{-1}correlates to the O–H Stretching vibration [45, 46]. The band around 1513–1516 cm^{-1} reflects the bending vibration of functional groups C–H [47]. The thin band at 1269–1278 cm^{-1}displays the alcohol functional groups

Table 1 Shows comparison of XRD datas of TiO_2 NPs with standard value

Standard datas (2θ)	Green synthesis (2θ)	Chemical synthesis (2θ)	Miller plane (h k l)
27.49	27.45	27.27	(1 1 0)
36.15	36.75	35.91	(1 0 1)
41.328	41.27	41.10	(1 1 1)
44.326	44.07	43.88	(2 1 0)
54.44	54.27	54.17	(2 1 1)
56.75	56.54	56.49	(2 0 0)
62.89	62.78	62.63	(0 0 2)
64.19	64.05	63.98	(3 1 0)
69.16	69.01	68.84	(3 0 1)
69.59	69.85	69.63	(1 1 2)

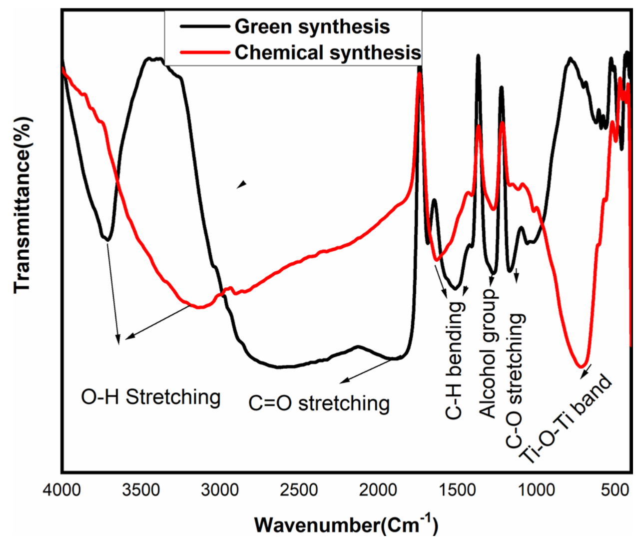

Fig. 2 Shows FT–IR spectra of TiO_2 nanoparticles

[48]. The band assigned at 1057–1055 cm^{-1} corresponds to C–O groups of aromatic stretching vibration. The strong band at 460 cm^{-1} and 900 cm^{-1} reveals the formation of Ti–O and Ti–O-Ti bending vibrations, respectively [49]. Peaks observed at 460–1000 cm^{-1} may disappear/partially decrease in intensity by annealing temperature [50]. The metal oxide bonds like Ti–O–Ti and Ti–O confirms the existence of TiO_2 in the prepared TiO_2 NPs. The presence of the Ti–O–Ti bond is due to the strong interaction (capped) of biomolecules with TiO_2 NPs which results in the presence of alkaloids, coumarins, flavonoids, tannins, and terpenoids [51]. These phytochemicals are responsible for reducing the bulk of titanium dioxide to stable TiO_2 in green synthesis [39]. The hydroxyl groups present at 3709–3712 cm^{-1} in TiO_2 NPs, which enhances the photocatalytic performance. The IR frequency of green synthesized TiO_2 NPs are slightly changed compared to chemically prepared TiO_2 NPs. The Band assignment corresponds to tentative frequency was tabulated in Table 2.

3.3 UV–Visible spectroscopy

The optical behavior of the TiO_2 NPs was investigated using the DRS spectrum. The UV–Visible reflectance spectrum of TiO_2 NPs was shown in Fig. 3. The spectra of TiO_2 NPs at 385 nm indicate the charge coordinated electronic transition between the O 2p state and Ti at 3d state [52]. During the biosynthesis process, the colloidal solution turns from white to yellowish-grey, which indicates the formation of titanium dioxide nanoparticles. The white colour dispersion shows the formation of TiO_2 NPs during the chemical process. The sharp absorption peak corresponds to the change in the crystalline

Table 2 Shows the FT-IR tentative frequency of TiO_2 nanoparticles

S.NO	Wave number (Cm^{-1})	Band assignment
1	3709–3712 Cm^{-1}	O–H stretching vibration
2	1513–1516 Cm^{-1}	Bending vibration of functional groups C–H
3	1269–1278 Cm-1	Alcohol groups
4	1057–1055 Cm-1	C–O groups of aromatic stretching vibration
5	460 and 900 Cm^{-1}	Ti–O and Ti–O–Ti bending vibrations

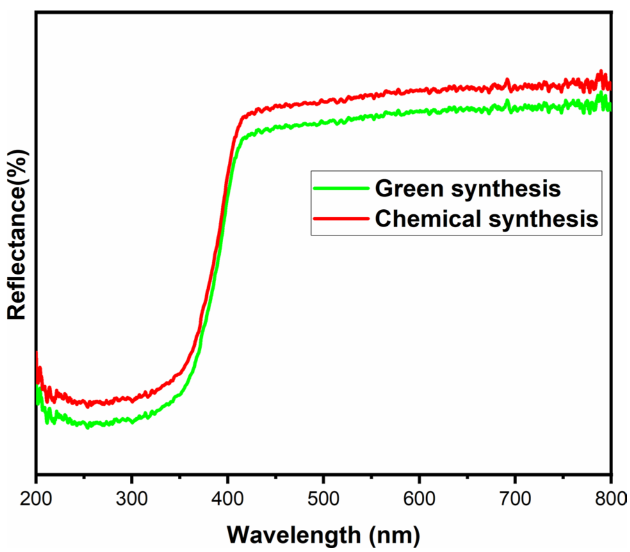

Fig. 3 Shows UV–Visible reflectance spectrum of TiO_2 nanoparticles

phase and the average crystalline size [53]. Hence the investigated nanomaterial is applicable for catalytic application [54, 55]. The sharp absorbance peak around 385–400 nm region confirms the formation of TiO_2 NPs. The reflectance spectra of TiO_2 NPs were well matched with the previous reports [56].

3.4 Scanning electron microscope

Figure 4 a, b, c, d shows the SEM images of prepared TiO_2 NPs. The SEM image of bio-mediated TiO_2 nanoparticles is a spherical shaped structure and the chemical synthesis TiO_2 nanoparticles sphere-like surface morphology. The average particle size of a spherical shaped TiO_2 NPs was found in the range of 32–48 nm. The Particle size obtained from SEM results is well correlated with the average crystalline size from XRD. In general, the decrease in particle size is inversely proportional to the surface volume of the material. Therefore the lower particle size material quickly penetrates the toxic elements as well as the bacterial surface that led the process of decomposition [57, 58].

3.5 Elemental dispersive spectrum

The elemental analysis of the chemical compounds was investigated through EDS spectra. Figure 5 shows the EDS spectra of Bio-mediated TiO_2 NPs. The elements present in the synthesized TiO_2 NPs are Titanium (Ti), and Oxygen (O) [59]. In bio-mediated TiO_2 NPs, the composition of the titanium element is high compared to oxygen content. The atomic and weight percentage of the TiO_2 NPs are tabulated in Table 3.

3.6 Anti-bacterial activity

The antibacterial study of TiO_2 nanoparticles was examined by gram-positive and gram-negative bacteria. Figure 6a, b shows anti bacterial activity of titanium dioxide nanoparticles. The cell wall of the gram-negative bacteria is composed of thin peptidoglycan and a thick layer of peptidoglycan in gram-positive bacteria. The zone inhibition layer of the TiO_2 NPs was examined against *Escherichia coli*, *Staphylococcus aureus*, and *Klebsiella pneumoniae*, which is measured in mm scale. Microbial pathogens may causes multiple diseases to living species. The zone inhibition layer for gram-negative bacteria such as E-Coli and Klebsiella are 12 and 11 mm for chemical synthesis and, 14 and 12 mm for green synthesis, respectively. At the same time, the zone inhibition layer for gram-positive microbial pathogens like staphylococcus aureus is 8 and 7 mm for green and chemical synthesis process. The high zone inhibition layer was observed in green synthesized TiO_2 NPs. The zone inhibition layer of pathogenic bacteria *Escherichia coli* and *Klebsiella pneumonia* have strong outcomes relative to *Staphylococcus aureus*. Thin walls of gram-negative bacteria are quickly broken by a positive ion of TiO_2 NPs. The Electrostatic interaction exists between the positive TiO_2 NPs and the negatively charged cell wall surface of *E.coli* and *Klebsiella pneumoniae*bacteria which leads to a high inhibition region on gram-negative bacteria. Bacterial cell walls induced by reactive oxygen species (ROS), such as hydroxyl group and superoxide result in a rupture on the bacterial cell wall. As the surface area of nanoparticles increases, there is an increase in surface oxide ion concentration and resulted in more effective

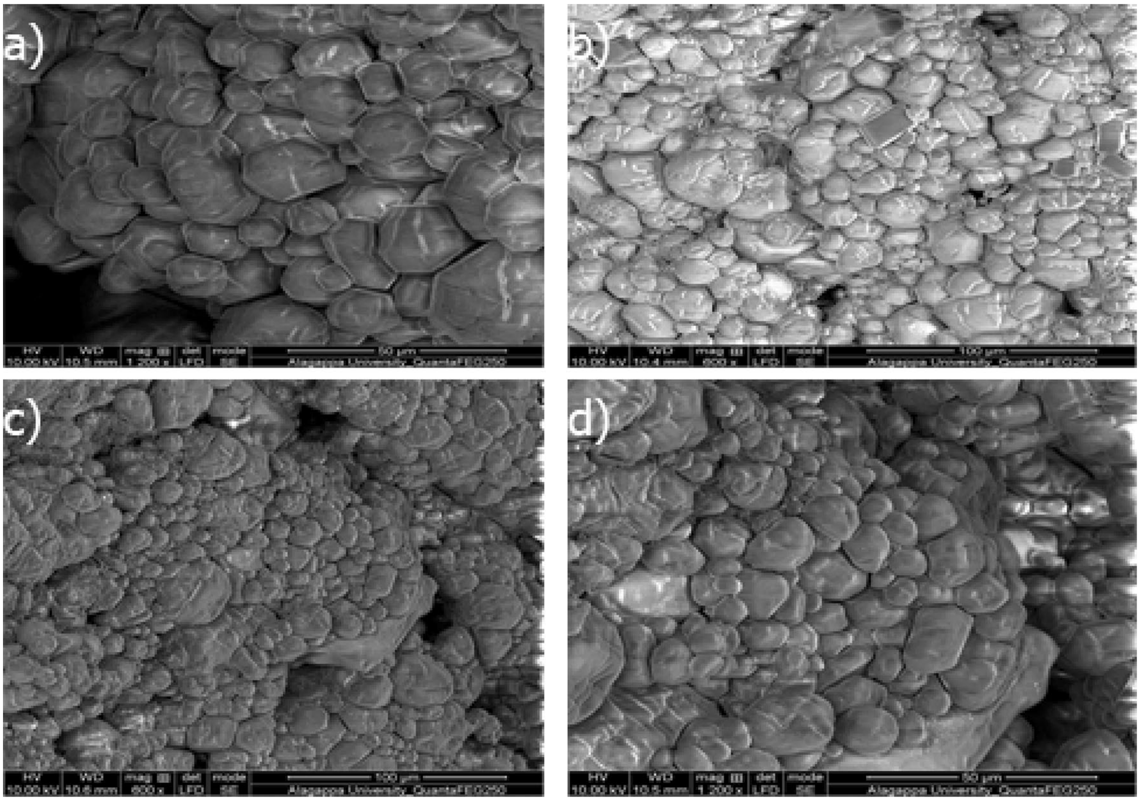

Fig. 4 Shows SEM images of TiO_2 nanoparticles at various magnification **a** and **b** Green synthesis method **c** and **d** Chemical method

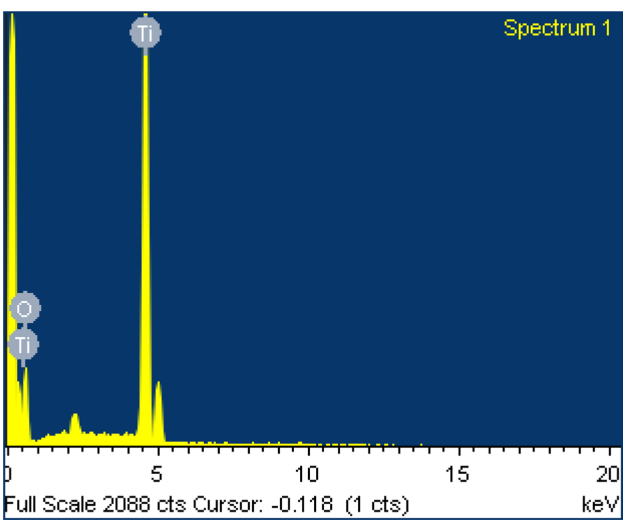

Fig. 5 Shows EDS spectra of TiO_2 NPs (green synthesis)

Table 3 Shows the elemental composition of TiO_2 nanoparticles green synthesis

s.no	Element	Weight (%)
1	Ti	55.12
2	O	44.88

destruction of the cytoplasm membrane and the cell wall of bacteria [60].

In this present report, gram-negative bacteria are highly potent when compared with gram-positive bacteria. The difference in diameter of zone of inhibition is due to the difference in susceptibility of bacteria, the morphology of nanoparticles, phase formations, particle size, shape, and synthesis method. The effect of inhibition of growth on both positive and negative bacteria owing to its vigorous antibacterial activity [61, 62]. The zone of inhibition (ZOI) of prepared TiO_2 NPs shows an excellent antibacterial activity. Thus, the prepared TiO_2 NPs are highly applicable to biomedical applications. The efficient antimicrobial agents must be poisonous to pathogens with the capability to be covered as antimicrobial coverings on medical appliances, purity testing devices, wound dressings, textiles, biomaterials, consumer products, food packaging [63].

3.7 Photocatalytic activity

The photodegradation of methylene blue dye was studied with the help of UV–Visible irradiation technique. Figure 7a, b shows the schematic representation of the photodegradation of methylene blue. The Photodegradation

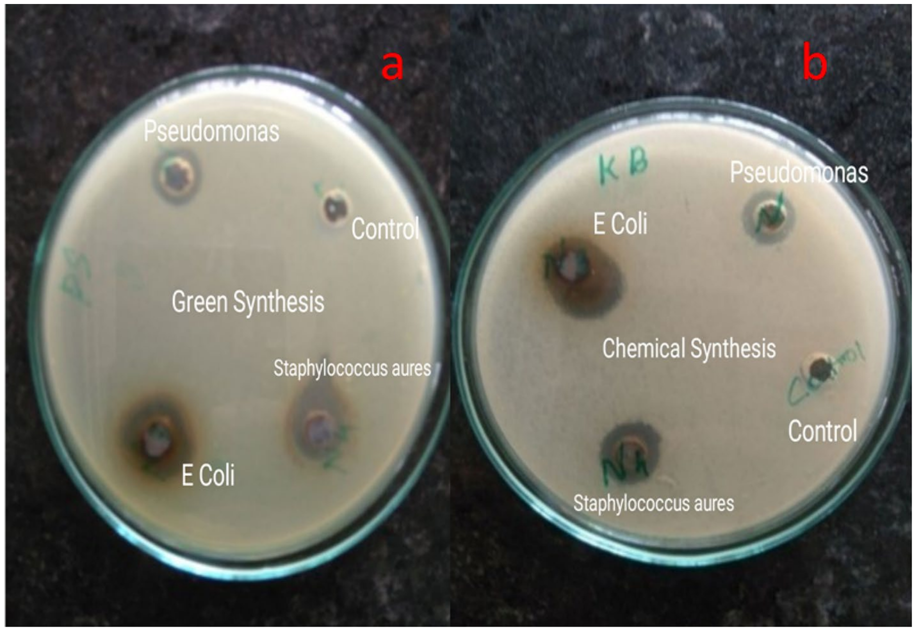

Fig. 6 Shows anti-bacterial activity of TiO_2 nanoparticles **a** Green synthesis method, **b** chemical method

efficiency of TiO_2 NPs was calculated using the following equation.

$$\text{Dye removal}(\%) = \frac{C_0 - C_t}{C_0} \times 100$$

where C_t is the temporal concentration of MB at time t and C_0 is the initial concentration of MB [64].

Photocatalytic activity of chemically and bio-mediated TiO_2 NPs were examined by methylene blue. In this study, methylene blue dye is used as a pollutant because it is widely utilized in the textile industry for colouring purposes, and also it is more harmful to human beings. So, the removal of methylene blue from wastewater is a challenging problem [65]. The photodegradation efficiency and the absorption spectra of methylene blue dye with a regular interval of time, as shown in Fig. 7a, b. The UV absorption spectra of methylene blue at 665 nm corresponds to π–π^* transition. Absorption peak intensity reduction results indicate the degradation of methylene blue. The Biologically synthesized TiO_2 NPs have higher degradation efficiency compared to chemically synthesized TiO_2 NPs. The degradation efficiency increases due to the presence of the hydroxyl group in jasmine flower extract. Bio mediated TiO_2 NPs results in the maximum degradation of 89% under 120 min of irradiation. When TiO_2 NPs undergo UV–Visible irradiation, the electron–hole pair is generated. The positive holes of TiO_2 NPs break water molecules to form hydrogen gas/free radical and negative electron react with oxygen molecules to form superoxide anions [66]. The electron–hole pair results in the formation of a hydroxyl group ($OH^{\cdot}$) and superoxide's ($O_2^{\cdot-}$). These superoxide's and hydroxyl groups are responsible for the degradation of methylene blue [67]. During the reduction process, methylene blue is converted to Leuco methylene blue (LMB) [68]. The degradation efficiency of bio-mediated TiO_2 and chemically investigated TiO_2 NPs are 89% and 82% respectively.

4 Conclusion

In this present work, TiO_2 NPs are successfully synthesized by green synthesis and hydrothermal method (chemical method). Colour changes confirmed the reduction of bulk Titanium to nanoparticles. The photodegradation of methylene blue under UV–Visible irradiation results in the degradation of methylene blue to leuco methylene blue. Bio-mediated TiO_2 shows maximum degradation efficiency of 89% under 120 min of irradiation. SEM image reveals that a uniform spherical shape surface morphology. The antibacterial activity of TiO_2 NPs was visualized by the agar diffusion method. Antibacterial activity of TiO_2 NPs was tested against bacterial pathogens such as Staphylococcus aureus (gram-positive bacteria) Escherichia coli and Klebsiella pneumonia (gram-negative bacteria). The bio-mediated TiO_2 NPs exhibit a good potent on antibacterial activity. The suggested results have inferred the property of TiO_2 nanoparticles is suited for biomedical and wastewater treatment (dye degradation) applications.

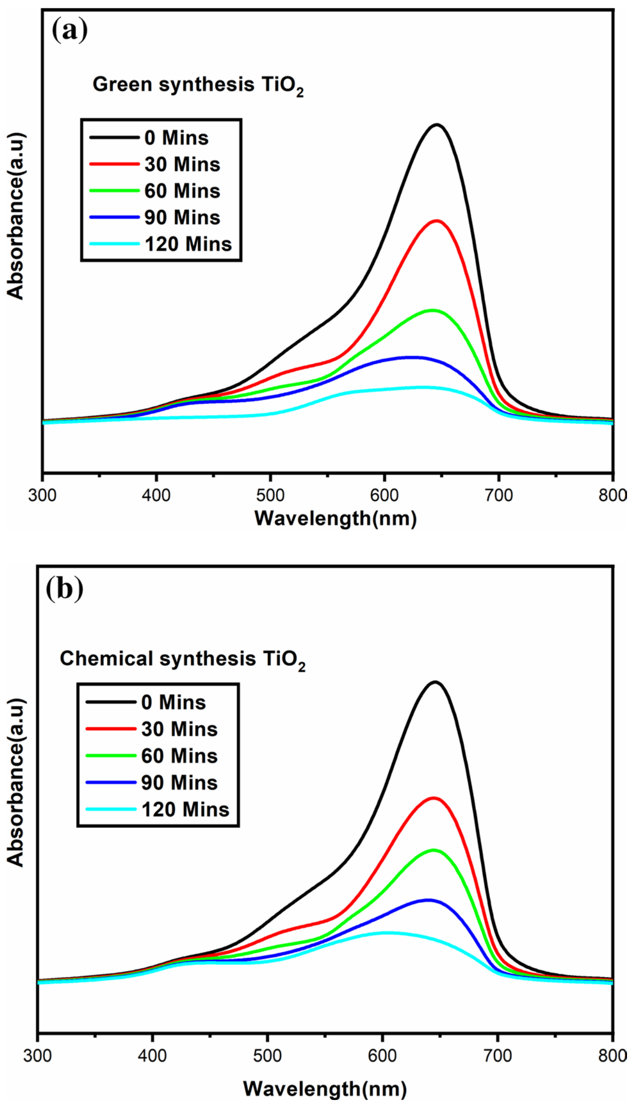

Fig. 7 Shows photocatalytic activity of TiO_2 NPs Green synthesis method, and chemical synthesis method

Compliance with ethical standards

Conflict of interest The authors declare that they have no conflict of interest.

References

1. Gebre SH, Sendeku MG (2019) New frontiers in the biosynthesis of metal oxide nanoparticles and their environmental applications: an overview. SN ApplSci 1(8):928
2. Hemalatha K, Madhumitha G, Kajbafvala A, Anupama N, Sompalle R, MohanaRoopan S (2013) Function of nanocatalyst in chemistry of organic compounds revolution: an overview. J Nanomater 2013:341015. https://doi.org/10.1155/2013/341015
3. Roopan SM, Kumar SHS, Madhumitha G, Suthindhiran K (2015) Biogenic-production of SnO_2 nanoparticles and its cytotoxic effect against hepatocellular carcinoma cell line (HepG2). ApplBiochemBiotechnol 175(3):1567–1575
4. Helan V, Prince JJ, Al-Dhabi NA, Arasu MV, Ayeshamariam A, Madhumitha G, Roopan SM, Jayachandran M (2016) Neem leaves mediated preparation of NiO nanoparticles and its magnetization, coercivity and antibacterial analysis. Results Phys 6:712–718
5. Hussain I, Singh NB, Singh A, Singh H, Singh SC (2016) Green synthesis of nanoparticles and its potential application. Biotech Lett 38(4):545–560
6. Azar BE, Ramazani A, Fardood ST, Morsali A (2020) Green synthesis and characterization of ZnAl2O4@ ZnOnanocomposite and its environmental applications in rapid dye degradation. Optik 208:164129
7. TaghaviFardood S, Ramazani A, Moradnia F, Afshari Z, Ganjkhanlu S, YekkeZare F (2019) Green synthesis of ZnO nanoparticles via Sol-gel method and investigation of its application in solvent-free synthesis of 12-Aryl-tetrahydrobenzo [α] xanthene-11-one derivatives under microwave irradiation. ChemMethodol 3(6):696–706
8. TaghaviFardood S, Moradnia F, Moradi S, Forootan R, YekkeZare F, Heidari M (2019) Eco-friendly synthesis and characterization of α-Fe2O3 nanoparticles and study of their photocatalytic activity for degradation of Congo red dye. Nanochem Res 4(2):140–147
9. Nabi G, Raza W, Tahir MB (2020) Green synthesis of TiO 2 nanoparticle using cinnamon powder extract and the study of optical properties. J InorgOrganometPolym Mater 30(4):1425–1429
10. Honarmand MM, Mehr ME, Yarahmadi M, Siadati MH (2019) Effects of different surfactants on morphology of TiO_2 and Zr-doped TiO_2 nanoparticles and their applications in MB dye photocatalytic degradation. SN ApplSci 1(5):505
11. Arulalrasu MV (2019) Effect of organic capping agents on the optical and photocatalytic activity of mesoporous TiO_2 nanoparticles by sol–gel method. SN ApplSci 1(5):393
12. Abisharani JM, Devikala S, Kumar RD, Arthanareeswari M, Kamaraj P (2019) Green synthesis of TiO2 nanoparticles using *Cucurbita pepo* seeds extract. Mater Today Proc 14:302–307
13. Ragupathi C, Vijaya JJ, Narayanan S, Kennedy LJ, Ramakrishna S (2013) Catalytic properties of nanosized zinc aluminates prepared by green process using Opuntiadilenii haw plant extract. Chin J Catal 34(10):1951–1958
14. Hayashi H, Hakuta Y (2010) Hydrothermal synthesis of metal oxide nanoparticles in supercritical water. Materials 3(7):3794–3817
15. Patil SA, Shinde DV, Patil DV, Tehare KK, Jadhav VV, Lee JK, Mane-Shrestha RSNK, Han SH (2014) A simple, room temperature, solid-state synthesis route for metal oxide nanostructures. J Mater Chem A 2(33):13519–13526
16. Chava RK, Kang M (2017) Improving the photovoltaic conversion efficiency of ZnO based dye sensitized solar cells by indium doping. J Alloy Compd 692:67–76
17. Liu H, Xu J, Liu G, Wang M, Li J, Liu Y, Cui H (2018) Building an interpenetrating network of Ni (OH) 2/reduced graphene oxide composite by a sol–gel method. J Mater Sci 53(21):15118–15129

18. Reinke M, Ponomarev E, Kuzminykh Y, Hoffmann P (2015) Combinatorial characterization of TiO2 chemical vapor deposition utilizing titanium isopropoxide. ACS Comb Sci 17(7):413–420
19. Yue X, Xiang J, Chen J, Li H, Qiu Y, Yu X (2020) High surface area, high catalytic activity titanium dioxide aerogels prepared by solvothermal crystallization. J Mater SciTechnol 47:223–230
20. Stucchi M, Bianchi CL, Argirusis C, Pifferi V, Neppolian B, Cerrato G, Boffito DC (2018) Ultrasound assisted synthesis of Ag-decorated TiO_2 active in visible light. UltrasonSonochem 40:282–288
21. Devipriya D, Roopan SM (2017) Cissusquadrangularis mediated ecofriendly synthesis of copper oxide nanoparticles and its antifungal studies against Aspergillus Niger, Aspergillusflavus. Mater SciEng C 80:38–44
22. RuddarajuPammiAnkaruntukuPadavalaKolapalli LKSVNGSVSVRM (2020) A review on anti-bacterials to combat resistance: from ancient era of plants and metals to present and future perspectives of green nano technological combinations. Asian J Pharm Sci 15(1):42–59
23. Ming ZX, Li HJ (2008) Dynamic property evaluation of aluminum alloy 2519A by split Hopkinson pressure bar. Trans Nonferrous Met Soc China 18:1–5
24. Rajakumar G, Rahuman AA, Roopan SM, Chung IM, Anbarasan K, Karthikeyan V (2015) Efficacy of larvicidal activity of green synthesized titanium dioxide nanoparticles using Mangiferaindica extract against blood-feeding parasites. Parasitol Res 114(2):571–581
25. Tahir MB, Nabi G, Khalid NR, Rafique M (2018) Role of europium on WO_3 performance under visible-light for photocatalytic activity. Ceram Int 44(5):5705–5709
26. Sankar R, Rizwana K, Shivashangari KS, Ravikumar V (2015) Ultra-rapid photocatalytic activity of Azadirachtaindica engineered colloidal titanium dioxide nanoparticles. ApplNanosci 5(6):731–736
27. Nabi G, Khalid NR, Tahir MB, Rafique M, Rizwan M, Hussain S, Iqbal T, Majid A (2018) A review on novel eco-friendly green approach to synthesis TiO_2 nanoparticles using different extracts. J InorgOrganometPolym Mater 28(4):1552–1564
28. Jalill A, Raghad DH, Nuaman RS, Abd AN (2016) Biological synthesis of titanium dioxide nanoparticles by *Curcuma longa* plant extract and study its biological properties. World Sci News 49(2):204–222
29. Roopan SM, Bharathi A, Prabhakarn A, Rahuman AA, Velayutham K, Rajakumar G, PadmajaLekshmi RDM, Madhumitha G (2012) Efficient phyto-synthesis and structural characterization of rutile TiO_2 nanoparticles using Annonasquamosa peel extract. SpectrochimActa Part A MolBiomolSpectrosc 98:86–90
30. Suman TY, Ravindranath RRS, Elumalai D, Kaleena PK, Ramkumar R, Perumal P, Aranganathan L, Chitrarasu PS (2015) Larvicidal activity of titanium dioxide nanoparticles synthesized using Morindacitrifolia root extract against Anopheles stephensi, Aedesaegypti and Culexquinquefasciatus and its other effect on non-target fish. Asian Pac J Trop Dis 5(3):224–230
31. Santhoshkumar T, Rahuman AA, Jayaseelan C, Rajakumar G, MarimuthuKirthiVelayuthamThomasVenkatesanKim SAVKJJSK (2014) Green synthesis of titanium dioxide nanoparticles using *Psidium guajava* extract and its antibacterial and antioxidant properties. Asian Pac J Trop Med 7(12):968–976
32. Fowsiya J, Madhumitha G, Al-Dhabi NA, Arasu MV (2016) Photocatalytic degradation of Congo red using *Carissa edulis* extract capped zinc oxide nanoparticles. J PhotochemPhotobiol B 162:395–401
33. Rajakumar G, Rahuman AA, Roopan SM, Khanna VG, Elango G, Kamaraj C, Zahir AA, Velayutham K (2012) Fungus-mediated biosynthesis and characterization of TiO2 nanoparticles and their activity against pathogenic bacteria. SpectrochimActa Part A MolBiomolSpectrosc 91:23–29
34. Rathore N, Kulshreshtha A, Shukla RK, Sharma D (2020) Study on morphological, structural and dielectric properties of sol-gel derived TiO_2nanocrystals annealed at different temperatures. Phys B 582:411969
35. Al-Snafi AE (2018) Pharmacology and medicinal properties of *Jasminum officinale*: a review. Indo Am J Pharm Sci 5(4):2191–2197
36. Keerthana BGT, Solaiyammal T, Muniyappan S, Murugakoothan P (2018) Hydrothermal synthesis and characterization of TiO_2 nanostructures prepared using different solvents. Mater Lett 220:20–23
37. Ahmad W, Jaiswal KK, Soni S (2020) Green synthesis of titanium dioxide (TiO_2) nanoparticles by using Mentha arvensis leaves extract and its antimicrobial properties. Inorg Nano-Metal Chem 50(10):1032–1038
38. Khalil AT, Ovais M, Ullah I, Ali M, Shinwari ZK, Maaza M (2020) Physical properties, biological applications and biocompatibility studies on biosynthesized single phase cobalt oxide (Co_3O_4) nanoparticles via Sageretiathea (Osbeck.). Arabian J Chem 13(1):606–619
39. Sundrarajan M, Bama K, Bhavani M, Jegatheeswaran S, Ambika S, Sangili A, Nithya P, Sumathi R (2017) Obtaining titanium dioxide nanoparticles with spherical shape and antimicrobial properties using *M. citrifolia* leaves extract by hydrothermal method. J PhotochemPhotobiol B 171:117–124
40. Moradnia F, Fardood ST, Ramazani A, Osali S, Abdolmaleki I (2020) Green sol–gel synthesis of CoMnCrO4 spinel nanoparticles and their photocatalytic application. Micro NanoLett 15(10):674–677
41. Moradnia F, Fardood ST, Ramazani A, Gupta VK (2020) Green synthesis of recyclable MgFeCrO4 spinel nanoparticles for rapid photodegradation of direct black 122 dye. J PhotochemPhotobiol A 392:112433
42. Kibasomba PM, Dhlamini S, Maaza M, Liu CP, Rashad MM, Rayan DA, Mwakikunga BW (2018) Strain and grain size of TiO_2 nanoparticles from TEM, Raman spectroscopy and XRD: the revisiting of the Williamson-Hall plot method. Results Phys 9:628–635
43. Hearne GR, Zhao J, Dawe AM, Pischedda V, Maaza M, Nieuwoudt MK, NemraouiCominsWitcomb OJDMJ (2004) Effect of grain size on structural transitions in anatase TiO_2: a Raman spectroscopy study at high pressure. Phys Rev B 70(13):134102
44. Karthik S, Siva P, Balu KS, Suriyaprabha R, Rajendran V, Maaza M (2017) Acalyphaindica–mediated green synthesis of ZnO nanostructures under differential thermal treatment: effect on textile coating, hydrophobicity, UV resistance, and antibacterial activity. Adv Powder Technol 28(12):3184–3194
45. Ba-Abbad MM, Kadhum AAH, Mohamad AB, Takriff MS, Sopian K (2012) Synthesis and catalytic activity of TiO_2 nanoparticles for photochemical oxidation of concentrated chlorophenols under direct solar radiation. Int J ElectrochemSci 7(6):4871–4888
46. Khalil AT, Ovais M, Ullah I, Ali M, Shinwari ZK, Hassan D, Maaza M (2018) Sageretiathea (Osbeck.) modulated biosynthesis of NiO nanoparticles and their in vitro pharmacognostic, antioxidant and cytotoxic potential. Artif Cells NanomedBiotechnol 46(4):838–852
47. Aisida SO, Madubuonu N, Alnasir MH, Ahmad I, Botha S, Maaza M, Ezema FI (2020) Biogenic synthesis of iron oxide nanorods using *Moringa oleifera* leaf extract for antibacterial applications. ApplNanosci 10(1):305–315
48. León A, Reuquen P, Garín C, Segura R, Vargas P, Zapata P, Orihuela PA (2017) FTIR and Raman characterization of TiO_2 nanoparticles coated with polyethylene glycol as carrier for 2-methoxyestradiol. ApplSci 7(1):49

49. Bagheri S, Shameli K, Abd Hamid SB (2013) Synthesis and characterization of anatase titanium dioxide nanoparticles using egg white solution via Sol–Gel method. J Chem 2013:1
50. Matinise N, Kaviyarasu K, Mongwaketsi N, Khamlich S, Kotsedi L, Mayedwa N, Maaza M (2018) Green synthesis of novel zinc iron oxide (ZnFe2O4) nanocomposite via MoringaOleifera natural extract for electrochemical applications. Appl Surf Sci 446:66–73
51. Mayedwa N, Mongwaketsi N, Khamlich S, Kaviyarasu K, Matinise N, Maaza M (2018) Green synthesis of nickel oxide, palladium and palladium oxide synthesized via *Aspalathus linearis* natural extracts: physical properties and mechanism of formation. Appl Surf Sci 446:266–272
52. Choudhury B, Dey M, Choudhury A (2013) Defect generation, d-d transition, and band gap reduction in Cu-doped TiO_2 nanoparticles. IntNanoLett 3(1):25
53. Fardood ST, Ramazani A, Joo SW (2017) Sol-gel synthesis and characterization of zinc oxide nanoparticles using black tea extract. J ApplChem Res 11(4):8–17
54. Fardood ST, Forootan R, Moradnia F, Afshari Z, Ramazani A (2020) Green synthesis, characterization, and photocatalytic activity of cobalt chromite spinel nanoparticles. Mater Res Express 7(1):015086
55. Moradnia F, Ramazani A, Fardood ST, Gouranlou F (2019) A novel green synthesis and characterization of tetragonal-spinel $MgMn_2O_4$ nanoparticles by tragacanth gel and studies of its photocatalytic activity for degradation of reactive blue 21 dye under visible light. Mater Res Express 6(7):075057
56. Vorontsov AV, Altynnikov AA, Savinov EN, Kurkin EN (2001) Correlation of TiO2 photocatalytic activity and diffuse reflectance spectra. J PhotochemPhotobiol A 144(2–3):193–196
57. Tulip DRE, Aishwarya KK, Surya KK, Krishna-Devi K, Kousalya R (2012) Biosynthesis of silver nanoparticles using Morindacitrifolia L. as capping and reducing agents. IJETT 3:24–34
58. Pal M, Garcia Serrano J, Santiago P, Pal U (2007) Size-controlled synthesis of spherical TiO_2 nanoparticles: morphology, crystallization, and phase transition. J PhysChem C 111(1):96–102
59. Venkatesh G, Geerthana M, Prabhu S, Ramesh R, Prabu KM (2020) Enhanced photocatalytic activity of reduced graphene oxide/$SrSnO_3$nanocomposite for aqueous organic pollutant degradation. Optik 206:164055
60. Bindhu MR, Umadevi M, Micheal MK, Arasu MV, Al-Dhabi NA (2016) Structural, morphological and optical properties of MgO nanoparticles for antibacterial applications. Mater Lett 166:19–22
61. Bindhu MR, Rekha PV, Umamaheswari T, Umadevi M (2014) Antibacterial activities of Hibiscus cannabinus stem-assisted silver and gold nanoparticles. Mater Lett 131:194–197
62. Fattahi FS, Zamani T (2020) Synthesis of polylactic acid nanoparticles for the novel biomedical applications: a scientific perspective. Nanochem Res 5(1):1–13
63. Bindhu MR, Umadevi M, Esmail GA, Al-Dhabi NA, Arasu MV (2020) Green synthesis and characterization of silver nanoparticles from *Moringa oleifera* flower and assessment of antimicrobial and sensing properties. J PhotochemPhotobiol B 205:111836
64. Singh S, Sidhu GK, Singh H (2019) Removal of methylene blue dye using activated carbon prepared from biowaste precursor. Indian ChemEng 61(1):28–39
65. Parvathiraja C, Shailajha S, Shanavas S, Mubina MK (2019) Photocatalytic and antibacterial activity of bio-treated Ag nanoparticles synthesized using Tinosporacordifolia leaf extract. J Mater Sci: Mater Electron 30(9):8515–8525
66. Palanisamy VK, Manoharan K, Raman K, Sundaram R (2020) Efficient sunlight-driven photocatalyticbehavior of zinc sulfidenanorods towards Rose Bengal degradation. J Mater Sci Mater Electron 31(17):14795–14809
67. Saufi H, El Alouani M, Alehyen S, El Achouri M, Aride J (2020) Photocatalytic degradation of methylene blue from aqueous medium onto perlite-based geopolymer. Int J Chem Eng 2020:9498349. https://doi.org/10.1155/2020/9498349
68. Naraginti S, Li Y (2017) Preliminary investigation of catalytic, antioxidant, anticancer and bactericidal activity of green synthesized silver and gold nanoparticles using *Actinidia deliciosa*. J PhotochemPhotobiol B 170:225–234